Isomerization and Decomposition of Indole. Experimental Results and Kinetic Modeling[†]

Alexander Laskin and Assa Lifshitz*

Department of Physical Chemistry, The Hebrew University, Jerusalem 91904, Israel

Received: June 2, 1997; In Final Form: July 18, 1997[⊗]

The thermal reactions of indole were studied behind reflected shocks in a pressurized driver single−pulse shock tube over the temperature range 1050−1650 K and densities of ~3×10^{-5} mol/cm^3. Similar to pyrrole, the main thermal reactions of indole are isomerizations. Three isomerization products are obtained under shock heating as a result of the pyrrole ring opening. These isomers are benzyl cyanide, *o*- and *m*-tolunitriles. Studies with toluene as a free-radical scavenger shows no effect on the production rates of these isomers. The decomposition products that were found in the postshock samples in decreasing order of abundance were C_2H_2, HCN, HC≡CCN, C_4H_2, C_6H_5CN, CH_3CN, and C_6H_6. Small quantities of C_6H_5−CH_3, CH_4, C_5H_5-CN, CH_2CHCN, C_5H_6, C_6H_5−C≡CH and traces of C_2H_4, CH_2=C=CH_2, CH_3−C≡CH, C_2H_4, C_6H_4, and C_5H_5−C≡CH were also found in the postshock mixtures. The total disappearance of indole in terms of a first-order rate constant is given by $k_{\text{total}} = 10^{15.78} \exp(-83.6 \times 10^3/RT)\text{s}^{-1}$ where R is expressed in units of cal/(K mol). At high temperatures the extent of fragmentation increases, and around 1300 K the fragmentation begins to exceeds that of the isomerizations. It is suggested that indole → benzyl cyanide isomerization starts with cleavage of the C(9)−N(1) bond followed by two 1,2 H-atom migrations. The mechanism of indole → tolunitrile isomerization involves a series of unimolecular steps which are preceded by the very fast indole ↔ indolenine tautomerism. The thermal decomposition of indole is initiated by H-atom ejection from the reactant. A reaction scheme containing 48 species 109 elementary reactions accounts for the observed product distribution. First-order Arrhenius rate parameters for the formation of the various reaction products are given, a reaction scheme is suggested, and results of computer simulation and sensitivity analysis are shown. Differences and similarities in the reactions of pyrrole and indole are discussed.

I. Introduction

The present investigation on the decomposition of indole is a part of an ongoing investigation at The Hebrew University of Jerusalem on the decomposition of nitrogen containing aromatic compounds as prototypes of fuel nitrogen. Indole and quinoline are embedded in the structure of coal of many origins and forms and are known to be its major nitrogenous constituents.[1−3] The study of the thermal reactions of indole, quinoline, and other similar nitrogen containing compounds in a pyrolitic environment is thus a prerequisite for the study of coal combustion.

Indole is a pyrrole ring fused to benzene. Whereas the thermal decomposition of pyrrole was studied in detail at high temperatures,[4,5] the available data on the decomposition of indole is very scarce and qualitative in nature. We are aware of only one, rather old, study by Bruinsma et al.[6] as a part of a general flow reactor investigation of the decomposition of a large number of aromatic compounds. No data, however, were reported in this study on the distribution of isomerization and decomposition products in indole nor on their production mechanism. Only overall disappearance rate of the reactant and its Arrhenius parameters were reported for all the compounds that were studied.

From organic chemistry viewpoint there is a marked difference in the reactivity and in the reactive sites in pyrrole when the ring stands alone as compared to a pyrrole ring fused to benzene. The reactive site in indole when reactions with electrophillic reagents are concerned is C(3), whereas the most reactive sites in pyrrole are C(2) and C(5). This difference in the reactive sites was explained[7,8] by the existence of reactive

tautomers of both pyrrole (pyrrolenine) and indole (indolenine) in which the formation of sp^3 C−H bonds are in different locations in the ring.
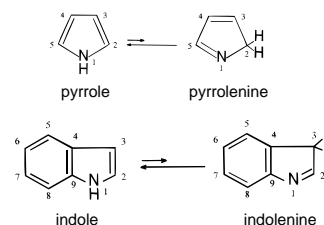
These two tautomers have not been isolated but derivatives corresponding to their structures are well-known[7,8] and thus support their existence.

As will be shown later, similar to pyrrole,[4,5] indole too isomerizes to various isomerization products in its main reaction channels. It also decomposes to fragment molecules in channels that increase rapidly with temperature.

In this investigation we describe the thermal reactions of indole and determine Arrhenius parameters for the formation of its isomerization and decomposition products. We also suggest a mechanism in which a preequilibrium between indole and indolenine is assumed; we compose a reaction scheme that describe the overall reaction and run computer simulation to support the suggested mechanism.

II. Experimental Section

Apparatus. The thermal reactions of indole were studied behind reflected shocks in a pressurized driver, 52-mm i.d. single-pulse shock tube, made of Double Tough Pyrex tubing. The tube and its gas-handling system were maintained at 150

± 1 °C. The heating system, which contained 15 independent heating ports, was computer controlled.

The 4-m long driven section was divided in the middle by a 52-mm i.d. ball valve. The driver had a variable length up to a maximum of 2.7 m and could be varied in small steps in order to obtain the best cooling conditions. Cooling rates were approximately 5×10^5 K/s. A 36-L dump tank was connected to the driven section at 45° angle near the diaphragm holder in order to prevent reflection of transmitted shocks and to reduce the final pressure in the tube. The driven section was separated from the driver section by Mylar polyester film of various thickness depending upon the desired shock strength.

Prior to performing an experiment, the tube and the gas-handling system were pumped down to ∼3×10^{-5} Torr. The reaction mixture was introduced into the driven section between the ball valve and the end plate, and pure argon into the section between the diaphragm and the valve, including the dump tank. After running an experiment, a gas sample was transferred from the tube, through a heated injection system, to a Hewlett-Packard Model 5890A gas chromatograph operating with a flame ionization (FID) and nitrogen phosphor (NPD) detectors.

Reflected shock temperatures were calculated in two different ways. In one series of experiments, the temperatures were calculated from the measured incident shock velocities using the three conservation equations and the ideal gas equation of state. The molar enthalpies of indole were taken from the thermodynamic compilations of McBride and Burcat.[9] In the other series, the reflected shock temperatures were calculated from the extent of decomposition of 1,1,1-trifluoroethane (CF_3-$CH_3 \rightarrow CF_2CH_2 + HF$) which was added in small quantities to the reaction mixture to serve as an internal standard. This decomposition is a first-order unimolecular reaction[10] with a rate constant equal to $k_{\text{first}} = 10^{14.51} \exp(-72.7 \times 10^3/RT)$ s^{-1}. Reflected shock temperatures in these series were calculated from the relation:

$$T = -(E/R)/\ln\left[-\frac{1}{At}\ln(1 - \chi)\right] \quad \text{(I)}$$

where E is the activation energy of the standard reaction, A is its preexponential factor, t is the reaction dwell time, and χ is the extent of decomposition defined as

$$\chi = [CF_2CH_2]_t/([CF_2CH_2]_t + [CF_3CH_3]_t) \quad \text{(II)}$$

The remaining reflected shock parameters were calculated from the measured incident shock velocities. These were measured with two miniature high-frequency pressure transducers (P. C. B. Model 113A26) placed 230 mm apart near the end plate of the driven section. The signals generated by the shock wave passing over the transducers were fed through an amplifier to a Nicolet Model 3091 digital oscilloscope. Time intervals between the two signals shown on the oscilloscope were obtained digitally with an accuracy of ±2 μs, corresponding to approximately ±20 K. A third transducer placed in the center of the end plate provided measurements of the reaction dwell time (approximately 2 ms) with an accuracy of ±5%.

Materials and Analysis. Reaction mixtures containing 0.3% indole and 0.3% indole + 0.05% 1,1,1-trifluoroethane diluted in argon were prepared in 12-L glass bulbs and stored at 150 ± 1 °C at a pressure of 700 Torr. Both the bulbs and the line were pumped down to approximately 10^{-5} Torr before the preparation of the mixtures. It should be mentioned that 2.1 Torr (0.3% of 700 Torr) of indole in the gas phase corresponds approximately to 15% of its equilibrium vapor pressure at 150 °C, thus the possible condensation of indole on the walls is
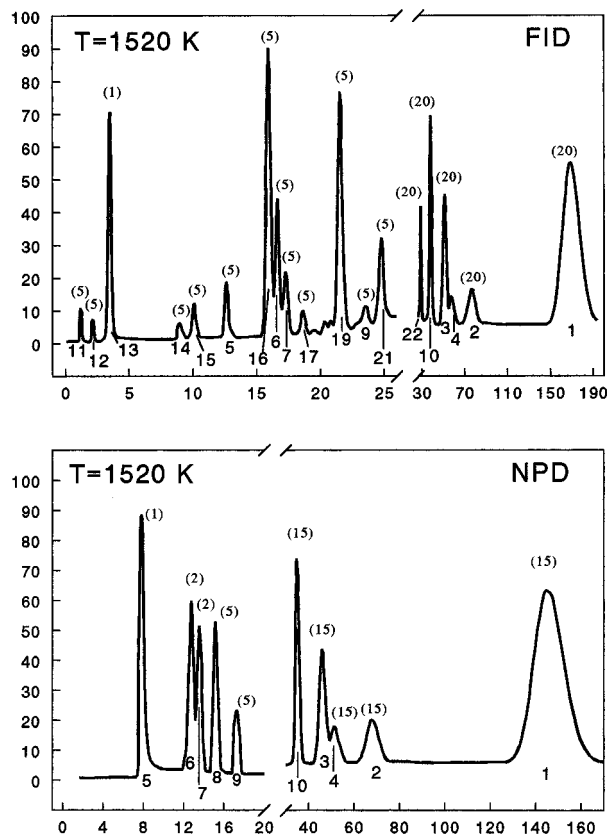

Figure 1. Gas chromatograms of a postshock mixture of 0.3% indole in argon taken on FID and NPD. The shock temperature is 1520 K. The numbers by the chromatogram peaks (in parentheses) indicate multiplication factors. The numbers below the chromatograms indicate the following compounds: (1) indole, (2) benzyl cyanide, (3) *o*-tolunitrile, (4) *m*-tolunitrile, (5) hydrogen cyanide, (6) cyanoacetylene, (7) acetonitrile, (8) acrylonitrile, (9) cyclopentadienyl cyanide, (10) benzonitrile, (11) methane, (12) ethylene, (13) acetylene, (14) allene, (15) propyne, (16) diacetylene, (17) cyclopentadiene, (19) benzene, (21) toluene, (22) phenylacetylene.

minimal. Indole, 99.0% pure, was obtained from Aldrich Chemical Co. and showed only one GC peak. 1,1,1-trifluoroethane, 99.0% pure, was obtained from P. C. R., Inc. and also showed only one GC peak. The argon used was Matheson ultrahigh purity grade, listed as 99.9995%, and the helium was Matheson pure grade, listed as 99.999%. All materials were used without further purification.

Gas chromatographic analyses of the postshock mixtures were performed on two 75 cm Porapak N columns with flame ionization and nitrogen phosphor detectors. Identification of the reaction products was based on their GC retention times and were also assisted by a Hewlett-Packard model 5970 mass selective detector. A typical FID and NPD chromatograms of a mixture of 0.3% indole in argon, shock-heated to 1520 K is shown in Figure 1.

The concentrations of the reaction products $C_5(\text{pr}_i)$ were calculated from their GC peak areas using the following relations:[11]

$$C_5(\text{pr}_i) = A(\text{pr}_i)/S_5(\text{pr}_i) \times \{C_5(\text{indole})_0/A(\text{indole})_0\} \quad \text{(III)}$$

$$C_5(\text{indole})_0 = \{p_1 \times (\%\text{indole})\rho_5/\rho_1\}/100RT_1 \quad \text{(IV)}$$

$$A(\text{indole})_0 = A(\text{indole})_t + (^1/_8)\Sigma N(\text{pr}_i)A(\text{pr}_i)_t/S(\text{pr}_i) \quad \text{(V)}$$

In these relations, $C_5(\text{indole})_0$ is the concentration of indole behind the reflected shock prior to decomposition and $A(\text{indole})_0$
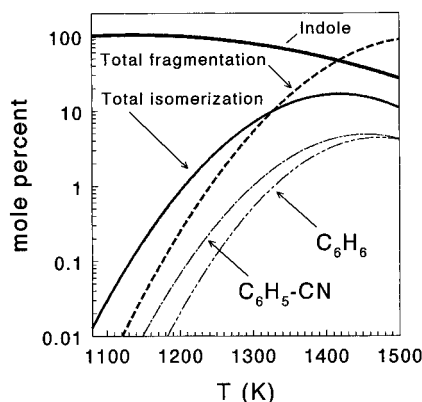
Isomerization and Decomposition of Indole

J. Phys. Chem. A, Vol. 101, No. 42, 1997 **7789**

Figure 2. Product distribution in the decomposition of indole showing the overall concentration of the isomerization products compare to the extent of fragmentation.
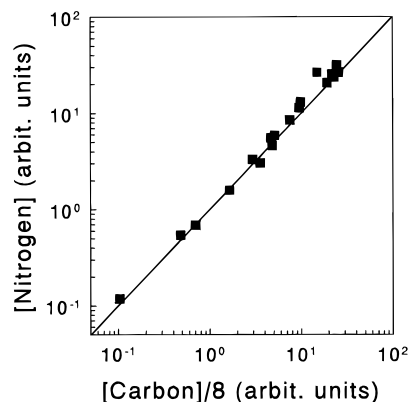

Figure 3. Nitrogen−carbon mass balance among the decomposition products.

is the calculated GC peak area of indole prior to decomposition (eq V) where $A(\text{pr}_i)_t$ is the peak area of a product i in the shocked sample, $S(\text{pr}_i)$ is its sensitivity relative to that of indole, $N(\text{pr}_i)$ is the number of its carbon atoms, ρ_5/ρ_1 is the compression behind the reflected shock, and T_1 is the initial temperature, equal to 423 K in the present series of experiments.

The sensitivities of the products to the FID and NPD were determined relative to indole from standard mixtures and were estimated for the following species: C_4H_2, $HC\equiv C-CN$, C_5H_5-CN, $C_5H_5-C\equiv CH$, based on comparison with the relative sensitivities of similar compounds. The areas under the GC peaks were integrated with a Spectra Physics Model SP4200 computing integrator and were transferred after each analysis to a PC for data reduction and graphical presentation.

III. Results

To determine the product distribution in the thermal reactions of indole and the Arrhenius parameters for their production rates, some 55 experiments were carried out, covering the temperature range 1050−1650 K at overall densities of ∼3 × 10⁻⁵ mol/cm³. The experiments were carried out with 1,1,1-trifluoroethane as an internal standard except for the high-temperature tests where the decomposition of the latter is no longer a simple unimolecular process. Several experiments were carried out in the presence of a large excess of toluene, which served as a free radical scavenger. These experiments were carried out in order to verify that the production of the isomerization products does not involve free radical reactions.

Details of the experimental conditions and the product distribution are given in Table 1. The mole percents given in the table correspond to the products' mole percent in the
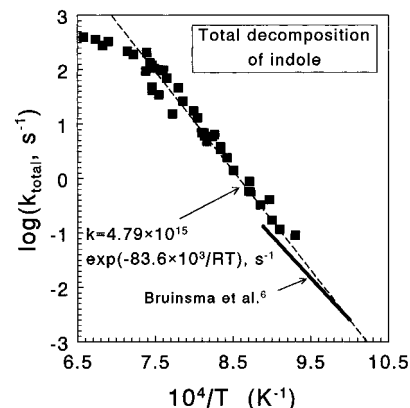

Figure 4. First-order Arrhenius plot of the rate constant for the overall disappearance of indole. Low-temperature rate constant ($k_{total} = 1.49 \times 10^{10} \exp(-57.0 \times 10^3/RT)$, s⁻¹), obtained by Bruinsma et al.,[6] is shown for comparison.

postshock mixture irrespective of the number of their carbon atoms. Molecular hydrogen is not included in the table.

There are three isomerization products, benzyl cyanide, *o*-tolunitrile, and *m*-tolunitrile. They are the major reaction products at low temperatures (at least two out of the three), but the fragmentation of indole to small molecular fragments becomes more important as the temperature increases. At 1400 K the concentration of the decomposition products exceeds that of the isomerization products. Figure 2 shows the extent of isomerization compared to fragmentation. The decomposition products found in the postshock mixtures in order of decreasing abundance were C_2H_2, HCN, $HC\equiv C-CN$, C_4H_2, C_6H_5-CN, CH_3-CN, C_6H_6 as major products and $C_6H_5-CH_3$, CH_4, C_5H_5-CN, CH_2CH-CN, C_5H_6, $C_6H_5-C\equiv CH$ as minor products. Traces of C_2H_4, $CH_2=C=CH_2$, $CH_3-C\equiv CH$, C_4H_4, C_6H_4, and $C_5H_4-C\equiv CH$ were also found in the postshock mixtures.

The balance of nitrogen vs carbon is shown in Figure 3. The concentrations of the nitrogen containing species are plotted against one-eighth the sum of the concentrations of all the decomposition products, each multiplied by the number of its carbon atoms. The 45° line in the figure represents a complete mass balance. As can be seen, within the limit of the experimental scatter, there is no major deviation from a nitrogen−carbon balance. The figure contains only the high-temperature data points since there is almost no decomposition at the low end of the temperature range.

Figure 4 shows an Arrhenius plot of the overall decomposition of indole calculated as a first-order rate constant from the relation:

$$k_{total} = -\ln([\text{indole}]_t/[\text{indole}]_0)/t \qquad (\text{VI})$$

The value obtained is $k_{total} = 10^{15.68} \exp(-83.6 \times 10^3/RT)$ s⁻¹ where R is expressed in units of cal/(K mol). The value obtained by Bruinsma et al.[6] in a low-temperature study is also shown for comparison. As can be seen there is a good agreement between the values of the rate constants in the two studies on the basis of an extrapolation of the data of the present study to the low temperatures of Bruinsma. The activation energy in the low temperature study is lower, probably owing to heterogeneous catalysis.

Three isomerization products of indole are formed when the latter is elevated to high temperatures. They are in decreasing order of abundance: benzyl cyanide and *o*- and *m*-tulonitriles. Figures 5−7 show Arrhenius plots of the first-order rate

7790 *J. Phys. Chem. A, Vol. 101, No. 42, 1997*

Laskin and Lifshitz

TABLE 1: Experimental Conditions and Product Distribution in Mole Percent of Nitrogen-Containing Species and of Hydrocarbons

						Nitrogen-Containing Species					
T_5, (K)	$C_5{}^a$	indole (1)^b	BC (2)	o-TN (3)	m-TN (4)	HCN (5)	HCCCN (6)	CH_3CN (7)	C_2H_3CN (8)	C_5H_4CN (9)	C_6H_5CN (10)
						T_5 calculated from shock speed measurements					
1210	3.31	98.72	0.91	0.360							
1225	3.31	99.05	0.696	0.258							
1230	3.33	98.10	1.051	0.313			0.004	0.051	0.024		0.069
1230	3.34	98.79	0.927	0.283							
1235	3.34	98.62	0.947	0.436							
1250	3.43	96.48	2.088	0.928			0.004	0.065	0.021	0.006	0.129
1280	3.52	90.90	4.396	2.050		0.074	0.034	0.189	0.055	0.047	0.314
1290	3.57	89.11	5.300	2.447		0.1390	0.055	0.198	0.049	0.043	0.454
1295	3.56	90.83	5.555	2.803	0.810						
1355	3.74	76.97	10.15	5.674	0.292		0.124	0.626	0.096	0.074	0.827
1385	3.80	57.50	15.03	10.38	1.133		0.470	1.396	0.192	0.185	2.552
1400	3.88	45.82	6.278	8.359	0.805	8.946	3.005	6.815	0.772	0.707	6.481
1450	4.01	27.94	3.980	5.044	1.563	10.09	3.532	5.552	1.115	0.117	4.202
1465	4.06	37.05	4.958	6.764	1.569	6.753	2.507	6.580	1.071	0.104	3.807
1485	4.10	27.05	4.464	5.929	1.646	7.632	3.038	6.486	1.263	0.116	4.468
1520	4.20	20.00	2.002	2.820	1.133	10.11	4.405	5.852	1.445	0.081	3.694
1555	4.29	15.82	0.879	0.977	0.463	13.17	5.056	4.470	1.203	0.038	2.067
1635	4.49	11.41	0.795	0.537	0.209	23.00	5.709	1.577	0.488		0.650
						T_5 calculated from the conversion of an internal standard					
1075	2.82	99.98	0.018								
1099	2.93	99.98	0.023								
1105	3.01	99.90	0.071	0.024				0.004	0.001		0.003
1111	2.93	99.97	0.035								
1115	2.93	99.92	0.064	0.018							
1130	2.98	99.93	0.059	0.007							
1146	3.07	99.89	0.088	0.024							
1148	3.07	99.79	0.112	0.051	0.007			0.004		0.002	0.011
1149	3.07	99.87	0.084	0.033				0.004			0.005
1175	3.17	99.72	0.216	0.064							
1187	3.21	99.52	0.397	0.083							
1199	3.25	99.23	0.593	0.173							
1199	3.25	99.25	0.519	0.155							0.073
1214	3.30	97.83	0.807	0.292			0.006	0.061	0.025	0.010	0.136
1243	3.39	96.06	1.599	0.615	0.106		0.024	0.074	0.027	0.038	0.308
1251	3.42	95.15	2.078	0.750	0.043	0.195	0.027	0.027	0.026	0.051	0.368
1273	3.49	92.23	2.522	1.186	0.066	0.441	0.063	0.111	0.053	0.127	0.913
1282	3.52	86.52	4.088	1.950	0.147	1.182	0.131	0.231	0.095	0.257	1.654
1307	3.60	80.41	5.408	2.972	0.239	2.114	0.271	0.473	0.150	0.360	2.482
1315	3.62	72.11	5.760	3.580	0.328	3.394	0.462	0.772	0.224	0.496	3.482
1315	3.62	77.67	8.398	5.392	0.342	0.586	0.111	0.753	0.106	0.160	1.353
1335	3.68	75.77	7.694	5.703	0.443	1.076	0.381	1.258	0.187	0.161	1.626
1340	3.71	71.55	8.911	6.360	0.569	2.007	0.392	1.261	0.184	0.219	1.950
1345	3.73	63.44	7.221	4.680	0.511	5.545	0.679	1.018	0.341	0.676	5.094
1353	3.74	54.97	10.73	9.220	1.063	8.987	0.833	2.826	0.459	0.261	3.053

				Hydrocarbons				
T_5 (K)	$C_5{}^a$	CH_4 (11)^b	C_2H_2 (13)	C_4H_2 (16)	C_5H_6 (17)	C_6H_6 (19)	$C_6H_5CH_3$ (21)	$C_6H_5C{\equiv}CH$ (22)
				T_5 calculated from shock speed measurements				
1210	3.31							
1225	3.31							
1230	3.33	0.222	0.078			0.025	0.010	
1230	3.34							
1235	3.34							
1250	3.43		0.155			0.073	0.035	
1280	3.52	0.423	0.474	0.008		0.148	0.108	
1290	3.57	0.418	0.446	0.055		0.194	0.126	0.033
1295	3.56							
1355	3.74	0.716	1.162	0.213	0.023	0.555	0.459	0.052
1385	3.80	0.928	3.333	0.846	0.032	1.308	0.876	0.087
1400	3.88	0.880	4.417	1.491	0.065	1.926	1.206	0.150
1450	4.01	1.866	17.43	7.404	0.253	3.664	1.457	0.415
1465	4.06	1.890	13.35	3.017	0.258	3.909	1.959	0.442
1485	4.10	2.511	16.35	7.659	0.273	4.364	1.879	0.546
1520	4.20	2.600	24.62	11.02	0.293	3.645	1.144	0.531
1555	4.29	2.470	32.63	13.51	0.229	2.453	0.440	0.399
1635	4.49	1.881	35.81	14.42	0.078	0.779	0.077	0.129

Isomerization and Decomposition of Indole

J. Phys. Chem. A, Vol. 101, No. 42, 1997 **7791**

TABLE 1 (Continued)

T_5 (K)	$C_5{}^a$	CH$_4$ (11)^b	C$_2$H$_2$ (13)	C$_4$H$_2$ (16)	C$_5$H$_6$ (17)	C$_6$H$_6$ (19)	C$_6$H$_5$CH$_3$ (21)	C$_6$H$_5$C≡CH (22)
				T_5 calculated from the conversion of an internal standard				
1075	2.82							
1099	2.93							
1105	3.01							
1111	2.93							
1115	2.93							
1130	2.98							
1146	3.07							
1148	3.07	0.011	0.002			0.002		
1149	3.07					0.002		
1175	3.17							
1187	3.21							
1199	3.25							
1199	3.25							
1214	3.30	0.244	0.188			0.077		
1243	3.39	0.355	0.055			0.038		
1251	3.42	0.323	0.059			0.205		
1273	3.49	0.349	0.408			0.528	0.046	
1282	3.52	0.507	0.629			0.863	0.150	0.011
1307	3.60	0.623	1.110	0.041		1.228	0.332	0.019
1315	3.62	0.915	2.368	0.089		2.237	0.528	0.044
1315	3.62	0.675	0.494	0.065		1.038	0.720	0.058
1335	3.68	0.876	1.012	0.097	0.056	1.366	0.872	0.100
1340	3.71	0.724	0.990	0.081	0.049	1.282	0.808	0.096
1345	3.73	0.998	2.402	0.112	0.102	2.476	0.739	0.080
1353	3.74	1.195	2.616	0.198	0.101	2.444	1.380	0.170
1187	3.21							
1199	3.25							
1199	3.25							
1214	3.30	0.244	0.188			0.077		

^{a} In units of 10^{-5} mol/cm^3. ^{b} The numbers in parentheses correspond to the peaks on the chromatograms (Fig. 1); BC, benzyl cyanide; o-TN, o-tolunitrile; m-TN, m-tolunitrile; C$_5$H$_4$CN, cyclopentadienyl cyanide; C$_6$H$_5$CN, benzonitrile; C$_5$H$_6$, cyclopentadiene; C$_6$H$_5$CH$_3$, toluene, C$_6$H$_5$C≡CH, phenylacetylene.
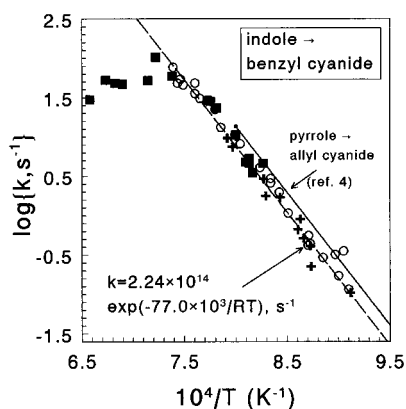

Figure 5. First-order Arrhenious plot for the production rate of benzyl cyanide. (○) experiments using an internal standard, (■) experiments using the measured shock speed for temperature calculations , (+) experiments with toluene as a free radicals scavenger); ref 4, the first-order rate constant for pyrrole → allyl cyanide isomerization obtained by Lifshitz et al.[4]

Figure 6. First-order Arrhenious plot for the production rate of o-tolunitrile. (○) experiments using an internal standard, (■) experiments using the measured shock speed for temperature calculations, (+) experiments with toluene as a free radicals scavenger.)

constants of their formation. They were calculated from the relation:

$$k_{product} = \frac{[product]_t}{[indole]_0 - [indole]_t} k_{total} \quad (VII)$$

Each figure contains the data from the three series of experiments including the one with the large excess of toluene (+). As can be seen, toluene has no effect on the rate of production of the isomerization products indicating that they are formed from indole by true unimolecular reactions without the involvement of free radicals. Figure 4 shows also the Arrhenius line for the pyrrole → allyl cyanide isomerization obtained by
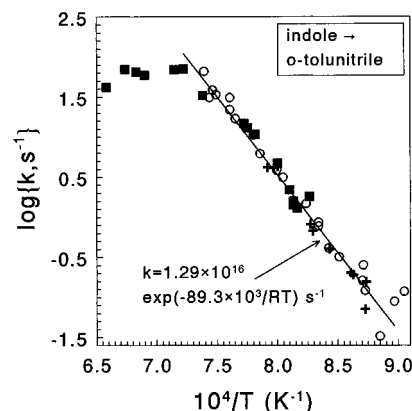
Lifsithz et al.[4] in their shock tube study of pyrrole decomposition. Figure 8 shows, as an example, Arrhenius plots of the first-order rate constants of formation of acetylene and phenyl acetylene.

Values of E obtained from the slopes of the lines and their corresponding preexponential factors are listed in Table 2 for the isomerization and the decomposition products. They were obtained from the low-medium conversion range in the figures before curvature begins to occur. The reason for this curvature, particularly in the Arrhenius plots of the isomers, is the decomposition of the products due to free radical reactions which become important at high temperatures. It should be mentioned that the Arrhenius parameters for the decomposition products do not represent elementary unimolecular reactions. They only represent formation rates.
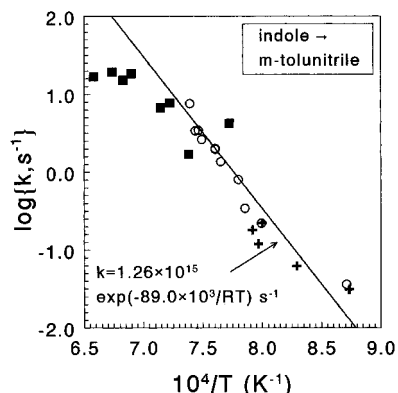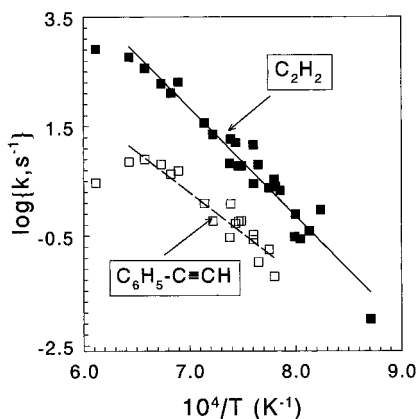
Figure 7. First-order Arrhenius plot for the production rate of *m*-tolunitrile. (○) experiments using an internal standard, (■) experiments using the measured shock speed for temperature calculations, (+) experiments with toluene as a free radicals scavenger.)
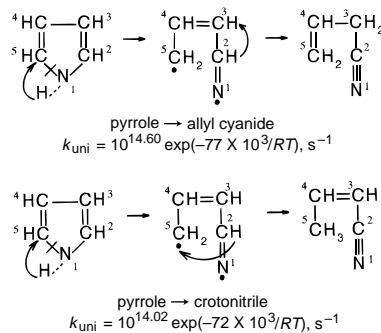

Figure 8. First-order Arrhenious plot for the production rate of acetylene and phenyl acetylene.

**TABLE 2: First-Order Arrhenius Parameters for Product Formation**

| compd	log $\{A, s^{-1}\}$	E (kcal/mol)	k (s^{-1}) (1250 K)	T (K)
total decomposition	15.68	83.0	1.47×10^1	1070−1330
benzyl cyanide	14.35	77.0	7.67	1070−1330
m-tolunitrile	16.11	89.3	3.13	1110−1370
o-tolunitrile	15.10	89.0	3.45×10^{-1}	1140−1370
HCN	15.91	91.4	8.48×10^{-1}	1210−1430
HC≡C−C≡N	19.49	117	9.16×10^{-2}	1210−1390
CH$_3$−C≡N	15.80	93.0	3.46×10^{-1}	1210−1390
CH$_2$=CH−C≡N	13.04	79.6	1.32×10^{-1}	1200−1390
C$_5$H$_4$−C≡N	12.67	76.7	1.81×10^{-1}	1140−1390
C$_6$H$_5$−C≡N	15.48	87.9	1.29	1140−1390
CH$_4$	11.64	66.7	9.49×10^{-1}	1140−1380
C$_2$H$_2$	15.65	90.2	7.55×10^{-1}	1140−1540
C$_4$H$_2$	15.21	96.5	2.17×10^{-1}	1300−1540
C$_6$H$_6$	15.50	87.6	1.52	1210−1430
C$_6$H$_5$−CH$_3$	17.77	106	2.10×10^{-1}	1210−1380
C$_6$H$_5$−C≡CH	10.75	68.8	5.25×10^{-1}	1280−1510

IV. The Reaction Mechanism

1. Isomerization Reactions. *A. Benzyl Cyanide.* The mechanism of formation of benzyl cyanide from indole can be viewed as an exact analogue of the pyrrole → allyl cyanide isomerization as suggested by Lifshitz et al.[4] in their study on the thermal reactions of pyrrole. Pyrrole isomerization was assumed to involve two consecutive steps: (1) cleavage of the C(5)−N(1) bond in the ring with a simultaneous 1,2 H-atom migration from nitrogen to carbon along the breaking bond and (2) a 1,2 H-atom migration from C(2) to C(3) to form allyl cyanide, or a 1,4 H-atom migration from C(2) to C(5) to form crotonitrile.

pyrrole → allyl cyanide
$k_{uni} = 10^{14.60} \exp(-77 \times 10^3/RT)$, s^{-1}

pyrrole → crotonitrile
$k_{uni} = 10^{14.02} \exp(-72 \times 10^3/RT)$, s^{-1}

The indole → benzyl cyanide isomerization, which is the main isomerization reaction in indole, can be described by a similar reaction mechanism. Cleavage of the C(9)−N(1) bond in the pyrrole ring with a simultaneous 1,2 H-atom migration from N(1) to C(9), followed by an additional 1,2 H-atom migration from C(2) to C(3), leads to the formation of benzyl cyanide.

indole → benzyl cyanide
$k_{uni} = 10^{14.35} \exp(-77 \times 10^3/RT)$, s^{-1}
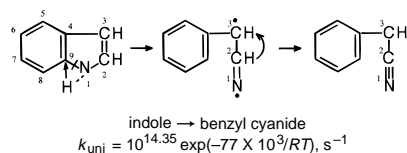
The benzene ring is not involved in this isomerization pathway. The C(2)−C(9) 1,4 H-atom migration that could form the analogue of crotonitrile does not occur, since it involves the formation of C(3)=C(4) double bond which destroys the aromaticity of the benzene ring, a process that requires additional 36 kcal/mol (resonance energy of the benzene ring).
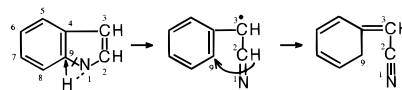
Since the degeneracy of the reaction pathway in pyrrole → allyl cyanide isomerization is 2, and in indole → benzyl cyanide isomerization it is 1 (cleavage of the C(2)−N(1) in the pyrrole ring will again destroy the benzene ring aromaticity), it is thus reasonable to expect that the preexponential factor for pyrrole → allyl cyanide isomerization would be approximately twice as high as the one for indole → benzyl cyanide isomerization. Indeed, the values of the preexponential factors obtained for the two molecules, using the same shock tube and under the same experimental conditions is $10^{14.35}$ s^{-1} for indole → benzyl cyanide and $10^{14.60}$ s^{-1} for pyrrole → allyl cyanide isomerization.[4]

To asses the extent of deviation of the deduced first-order rate constant for indole → benzyl cyanide from the high-pressure limit value, an RRKM calculation was ran. The RRKM calculation[12] uses Troe's formulation[13−15] of the second-order rate constant in the low-pressure limit.

The frequencies of the transition state were those of indole,[16] except for the frequency of the N(1)−C(9) stretch that was taken as the reaction coordinate and another four stretching frequencies: N(1)−C(2), C(2)=C(3), N(1)−H(1), and C(2)−H(2) were changed in the transition state. These frequencies were adjusted so that the experimental first-order rate constant of the benzyl cyanide production would be equal to the calculated unimolecular rate constant k_{uni} at the same pressure. $<\Delta E>_{down}$ and E_0 (the barrier) were taken as 400 cm^{-1} and 75.8 kcal/mol, respectively. We found that at 1070 K the ratio k_{uni}/k_∞ was 0.92 and, at 1330 K, 0.81. The first-order high-pressure limit rate constant was derived as: $k_\infty = 10^{14.66} \exp(-78.4 \times 10^3/$

RT) s^{-1}. It can be assumed that the ratio k_{uni}/k_∞ for the rate determining step in other isomerizations would be roughly the same.

B. o- and m-Tolunitrile. The suggested mechanism for the formation of *ortho* and *meta* toluitriles is more complicated than that of benzyl cyanide since it involves several consecutive unimolecular steps prior to the formation of the final isomerization product.

In their study on pyrrole isomerization, Mackie et al.[5] suggested that the transfer of a hydrogen atom from the nitrogen to C(2), which is necessary for the isomerization to take place, occurs via the very fast formation of the tautomeric compound pyrrolenine (C(2) is the most reactive site in pyrrole, see Introduction). Lifshitz et al.[4] suggested, on the other hand, a simultaneous N(1)−C(2) bond cleavage and N(1) → C(2) H-atom migration.

Whereas the assumption of the participation of a tautomer in the initial cleavage of the ring in pyrrole is more of a semantic nature, the fast attainment of an equilibrium between indole and indolenine, on the other hand, is necessary to explain the mechanism of formation of *o*- and *m*-tolunitrile. It take place via the following three steps:

1)   fast (in a state of thermal equilibrium)

2)   slow (rate determining step)

3)   fast
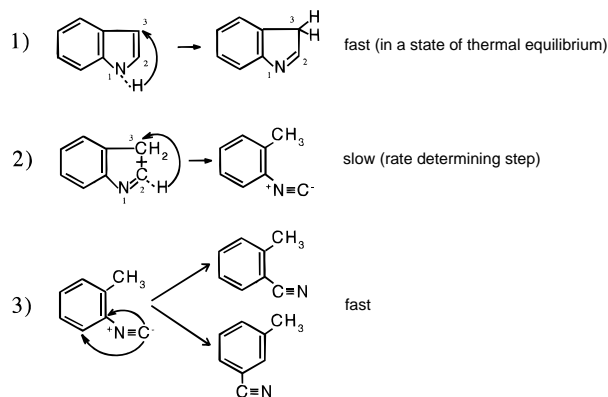
It should be mentioned that, in indole, in contradiction to pyrrole, the most reactive site in the pyrrole ring is C(3).[17] Cleavage of the C(2)−C(3) bond in indolenine with a simultaneous 1,2 H-atom migration from C(2) to C(3) forms *o*-toluil isocyanide. The very fast isocyanide−cyanide isomerization that follows can take place by a rearrangement of the isocyanide group on the same carbon atom in the ring to form *o*-tolunitrile. It can also rearrange on a neighboring carbon with 1,2 H-atom migration to form *m*-tolunitrile. The branching ratio between these two modes of rearrangement is in favor of the *ortho* isomer with a branching ratio of approximately 10:1 at 1200 K. Since the ratio decreases with temperature, the difference in the rates of the two processes is also owing to different activation energies.

p-Tolunitrile was not found in the postshock samples even after an intensive search. The isocyanide−cyanide group rearrangement is a concerted process and not a dissociation-recombination reaction. The distance to the next neighboring atom (*para* to the C−CH$_3$ carbon) is too big to allow the isocyanide−cyanide group rearrangement to take place. Thus, only two isomers of tulonitriles are obtained.
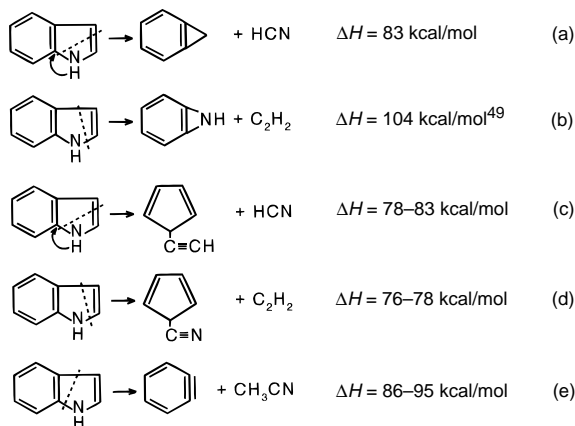
2. Decompositions. *A. Unimolecular Decomposition of Indole.* As indole is a pyrrole ring fused to benzene, it is of interest to examine similarities and differences in the decomposition pattern of the pyrrole ring in indole and in pyrrole. The common feature in the thermal reactions of these two molecules is the extent of isomerization vs decomposition and

its temperature dependence. In both molecules the isomerizations are the main channels that involve ring opening, and they are only slightly endothermic ($\Delta H_{react.} \approx 6-11$ kcal/mol). As the temperature increases the extent of ring destruction by decomposition to fragment molecules increases.[4,5] This has already been demonstrated for indole in Figure 2.

It has been shown that 5-membered heterocyclics, such as pyrrole,[4,5] furan,[18] oxazole,[19] isoxazole,[20] and others, and their substituted derivatives[21,22] undergo ring opening by breaking the (1)−(5) bond (or the (1)−(2) bond) in the molecule to produce either isomerization or decomposition products. In addition to this dominant channel, other unimolecular decomposition pathways were reported in the literature where the molecule splits into two stable fragments by concerted processes. Thus, in pyrrole for example, in addition to the channels that lead to isomerization, the following two channels were reported.[4,5]

     $C_2H_2 + CH_3CN$ $\Delta H = 47$ kcal/mol

 $HCN + CH_3C{\equiv}CH$ $\Delta H = 51$ kcal/mol
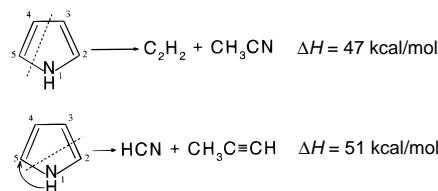
Owing to the combination of the benzene and pyrrole rings, the ring opening channels that can take place in pyrrole are not very likely to contribute much in indole owing to much higher endothermicity and thus higher activation energies. The reactions in pyrrole that involve cleavage of the ring and production of stable molecules such as CH$_3$CN + C$_2$H$_2$ and HCN + CH$_3$C≡CH, can take place in indole by either production of a three membered ring fused to benzene (a and b), by the formation of cyclopentadiene structures (c and d) or by the forming of benzyne (e).

     + HCN $\Delta H = 83$ kcal/mol   (a)

     NH + C$_2$H$_2$ $\Delta H = 104$ kcal/mol[49]   (b)

     + HCN $\Delta H = 78{-}83$ kcal/mol   (c)

     + C$_2$H$_2$ $\Delta H = 76{-}78$ kcal/mol   (d)

     + CH$_3$CN $\Delta H = 86{-}95$ kcal/mol   (e)

As can be seen in a−e, all of these channels are considerably more endothermic than the equivalent channels in pyrrole. Since the reverse reactions of these channels involve interactions between two stable molecules, they must also have reasonably high energy barriers. In view of the high endothermicity, the activation energies for the forward reactions of these channels must be very high and can thus contribute but very little to the decomposition of indole and to the production of the products in question. Compounds having $m/z = 90$ and 91 corresponding to 1-cyclopentadienecarbonitrile and 1-cyclopentadienylacetylene were indeed identified in the postshock mixtures in very small quantities, but we believe that their production involves a different mechanism, as will be shown later.

B. Free Radical Reactions. a. Initiation. It is believed that the channel in the decomposition of indole that involves a hydrogen atom ejection from the pyrrole ring is more important in the decomposition of indole than in that of pyrrole. In view of the very fast tautomerism indole → indolenine ($\Delta H_r^0(298)$ ~18 kcal/mol), equilibrium between the two tautomers is established as of the early stages of the reaction (computer simulation shows that full equilibrium is established approximately after 150−200 μs). The hydrogen atom can be ejected from either the nitrogen in the pyrrole ring ($D_{N-H} = 88$ kcal/mol) or from the sp^3 carbon in indolenine ($D_{CH-H} = 70$ kcal/mol).
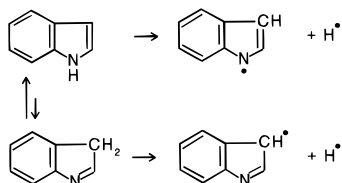
The final product of H-atom elimination from the molecule is identical whether the ejection takes place from indole or from indolenine. Since equilibrium is also maintained during almost the entire reaction time, the question from where precisely the ejection of the H atom takes place is imaterial from a kinetic viewpoint.

At higher temperatures, where the concentration of the isomerization products reaches significant value, H atoms can be also ejected from the sp^3 C−H bonds of the isomerization products, as follows:
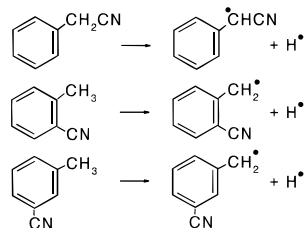

b. Free Radical Attack on Indole, Production of Benzene and Benzonitrile at Low Temperatures. The attack of hydrogen atoms on indole (or indolenine) is the major propargation reaction at low temperatures, where the reactant is still the most abundant component in the reaction mixture. The H-atom attack can take place by the abstraction of H atoms from the molecules, forming indolyl radical and a hydrogen molecule:
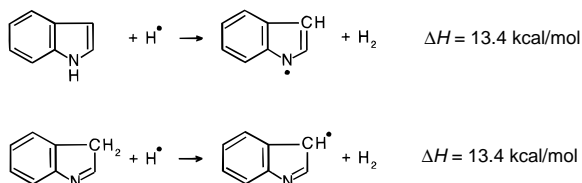

Dissociative attachments of H atoms on the reactant molecule were also introduced into the reaction scheme in order to describe the benzonitrile and benzene production at low temperatures.

As can be seen in Figure 2, at low temperatures practically only benzonitrile and benzene appear as decomposition products. The production of benzonitrile, for example, can in principle be described by an H-atom-induced methyl group displacement from the two isomers of tolunitrile.
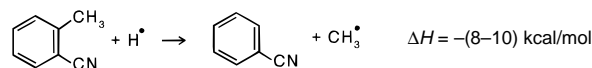

This process is very well-known in toluene.[23,24] However, in the low-temperature range of this investigation, the concentrations of the isomers are too small to serve as precursors for the formation of either benzonitrile or benzene. To account for their relatively large concentrations already at low temperatures, they must be formed from the reactant directly. We therefore suggest that both benzonitrile and benzene are formed by dissociative attachments of H atoms to indole to form either benzonitrile and methyl radical or benzene with cyanomethyl radical.
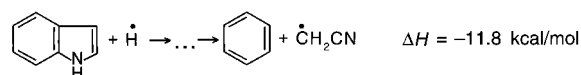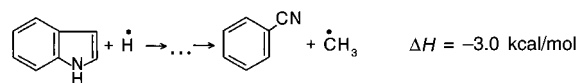

Since these processes involve two bond ruptures and several H-atom migrations in each reaction, they must occur in more than one step.

c. Free Radical Attack on the Isomerization Products. Free radical attack on the isomerization products of indole, benzyl cyanide, and *o*- and *m*-tolunitriles plays a central role in the reaction mechanism, since the concentrations of the latter reach high values before the fragmentation of indole begins to occur. Since H-atom ejection from pyrrole is the initiation reaction, hydrogen atoms are the first reactive free radicals in the system. There are three possible modes of H-atom attack on these isomers; abstraction of another H-atom from, dissociative attachment, and group displacement. These reaction channels will now be listed.

A hydrogen atoms can abstract a sp^3 hydrogen from the isomers, as the sp^3 C−H is the weakest bond.
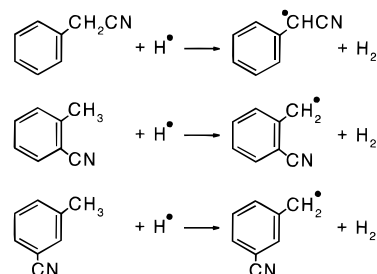
It can also attach to the −C≡N triple bond in the molecule with the displacement of HCN.
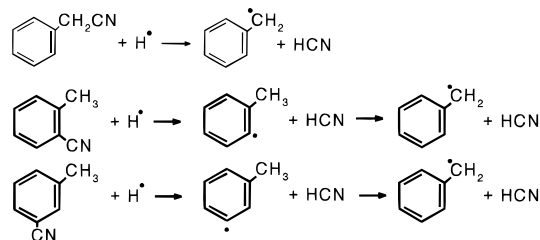
A process which is known to occur but at a somewhat lower rate is a group displacement. There are three different groups attached to the benzene ring in the isomers of indole. These are −CH$_2$CN, −CH$_3$, and −CN. The possible group displacements are
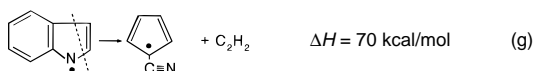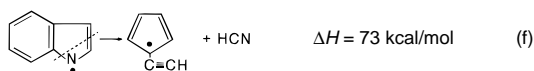
Isomerization and Decomposition of Indole

J. Phys. Chem. A, Vol. 101, No. 42, 1997 **7795**
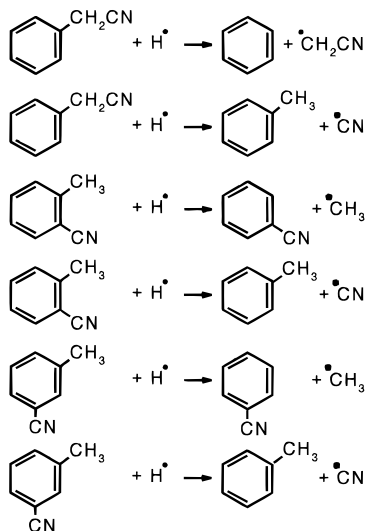
Whereas the only radical that plays an important role at the early stages of the fragmentation is H•, other radicals such as CN•, CH₃•, CH₂CN•, and C₃H₃• play a significant role at high temperatures.

d. **Thermal Reactions of Indolyl Radical Isomerizations and Decompositions.** Indolyl radicals are formed in the initiation process and by H-atom abstractions from indole. Their decompositions and isomerizations are important components of the overall decomposition of indole.

It is suggested that the isomerizations of the indolyl radical follow the same pattern of indole except that the production of benzylcyanide radical involves a 1,4 H-atom migration from C(2) to C(9), rather than a 1,2 H-atom migration from N(1) to C(9) as is indole:
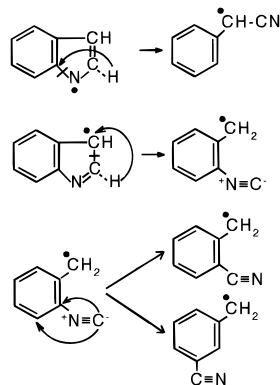
In contradiction to the indole molecule where the unimolecular decomposition pathways were neglected because of high barriers, the unimolecular decompositions of indolyl radical are more plausible and should be considered. There are two reasons why these should be taken into account: (1) The endothermicity, at least in two decomposition channels, f and g, is smaller than in all the channels of indole decomposition, and (2) since the back reactions of indolyl decomposition involve interactions of stable molecules with free radicals, their barriers are not as high as in indole where reactions between stable molecules is involved. We introduced channels f and g into the reaction scheme (Table 3).

$$+ \text{HCN} \qquad \Delta H = 73 \text{ kcal/mol} \qquad \text{(f)}$$

$$+ \text{C}_2\text{H}_2 \qquad \Delta H = 70 \text{ kcal/mol} \qquad \text{(g)}$$

e. **Decomposition of Benzyl Radical and Its Derivatives.** As has already been shown, a number benzyl radicals containing a −CN group in various locations in the molecule are formed during the decomposition of indole mainly as a result of H-atom abstraction from the isomers. Their decomposition channels play an important role in the process and are assumed to be similar to the decomposition of benzyl radical, a process that has been thoroughly investigated in the past.

Cyclopentadienyl radical and acetylene were reported as the major decomposition products of benzyl radicals.[25,26] According to the suggested mechanism,[27] benzyl radical isomerizes first to a bicyclopentadienyl intermediate, which then decomposes to cyclopentadienyl and acetylene. It should be mentioned, however, that there is no experimental evidence that could support this intermediate. Indeed, this process could be also viewed as proceeding via cycloheptatrienyl intermediate that is preferable from thermochemical viewpoint. The precise mechanism is beyond the scope of this investigation and we have described the process as a single step process. The thermal decomposition of the other benzyl derivatives were introduced into the reaction scheme in the same way as benzyl decomposition, where each one of them can proceed via two different pathways, depending upon the location of the cyanide group.
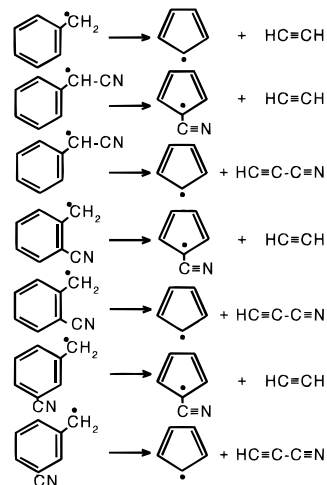
f. **Decomposition of Cyclopentadienyl Radical and Its Derivatives.** This group of radicals have also a common form, and as has been suggested, they undergo ring rupture similar to cyclopentadienyl.[28]
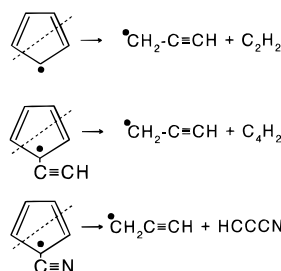
3. **Computer Modeling.** To account for the distribution of the isomerization and decomposition products, a reaction scheme based on the suggested mechanism containing 48 species and 109 elementary reactions was constructed. The scheme is shown in Table 3. The rate constants are given as $k = A \exp(-E/RT)$ in units of cm³, mol, s, kcal.

The Arrhenius rate parameters assigned for the unimolecular isomerizations (reactions 1 and 3) are based on experimental first order rate constants of the production of the isomers

TABLE 3: Reaction Scheme for the Decomposition of Indole (Values Are Given at 1300 K)[a]
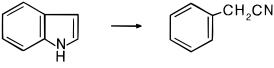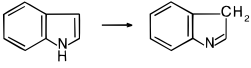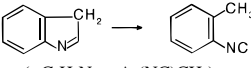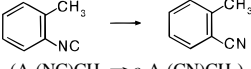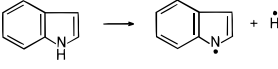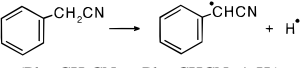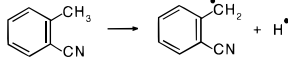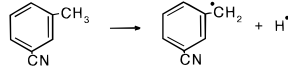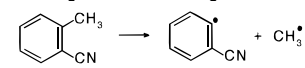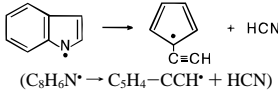
	reaction	A	E_{activ}	$\Delta S_r°$	$\Delta H_r°$	source
1.	$(C_8H_7N \rightarrow Ph-CH_2CN)$	2.25×10^{14}	77	8	4	present work
2.	$(C_8H_7N \rightarrow t\text{-}C_8H_7N)$	1×10^{12}	58	3	18	estimated[b]
3.	$(t\text{-}C_8H_7N \rightarrow A_1(NC)CH_3)$	8.0×10^{14}	67	5	11	present work
4.	$(A_1(NC)CH_3 \rightarrow o\text{-}A_1(CN)CH_3)$	6×10^{14}	41	−1	−23	estimated[c]
5.	$(A_1(NC)CH_3 \rightarrow m\text{-}A_1(CN)CH_3)$	8×10^{13}	52	−1	−24	estimated
6.	$(C_8H_7N \rightarrow C_8H_6N^\bullet + H^\bullet)$	3×10^{15}	84	34	89	estimated
7.	$(Ph-CH_2CN \rightarrow Ph-CHCN^\bullet + H^\bullet)$	3.1×10^{15}	89.2	33	88	estimated[d]
8.	$(o\text{-}A_1(CN)CH_3 \rightarrow o\text{-}A_1(CN)CH_2^\bullet + H^\bullet)$	3.1×10^{15}	89.2	33	91	estimated[d]
9.	$(m\text{-}A_1(CN)CH_3 \rightarrow m\text{-}A_1(CN)CH_2^\bullet + H^\bullet)$	3.1×10^{15}	89.2	33	91	estimated[d]
10.	$Ph-CH_2CN \rightarrow Ph + CH_2CN^\bullet$	2×10^{15}	93	40	93	estimated
11.	$(o\text{-}A_1(CN)CH_3 \rightarrow C_6H_4CN^\bullet + CH_3^\bullet)$	2×10^{15}	98	41	100	estimated
12.	$m\text{-}A_1(CN)CH_3 \rightarrow C_6H_4CN^\bullet + CH_3^\bullet$	2×10^{15}	98	41	101	estimated
13.	$H^\bullet + C_8H_7 \rightarrow C_8H_6N^\bullet + H_2$	4×10^{14}	9	6	−18	estimated
14.	$H^\bullet + C_8H_7N \rightarrow Ph-CN + CH_3^\bullet$	4×10^{14}	12	13	−7	estimated
15.	$H^\bullet + C_8H_7N \rightarrow C_6H_6 + CH_2CN^\bullet$	4×10^{14}	14	12	−15	estimated
16.	$CH_3^\bullet + C_8H_7N \rightarrow C_8H_6N^\bullet + CH_4$	5×10^{12}	9	−1	−19	estimated
17.	$CH_2CN^\bullet + C_8H_7N \rightarrow C_8H_6N^\bullet + CH_3CN$	1×10^{12}	9	−1	−5	estimated
18.	$C_3H_3^\bullet + C_8H_7N \rightarrow C_8H_6N^\bullet + C_3H_4$	1×10^{12}	9	1	−4	estimated
19.	$CN^\bullet + C_8H_7N \rightarrow C_8H_6N^\bullet$	1×10^{13}	3	4	−38	estimated
20.	$H^\bullet + Ph-CH_2CN \rightarrow Ph-CHCN^\bullet + H_2$	4.0×10^{14}	9.8	5	−19	estimated[e]
21.	$H^\bullet + o\text{-}A_1(CN)CH_3 \rightarrow o\text{-}A_1(CN)CH_2^\bullet + H_2$	4.0×10^{14}	9.8	6	−16	estimated[e]
22.	$H^\bullet + m\text{-}A_1(CN)CH_3 \rightarrow m\text{-}A_1(CN)CH_2^\bullet + H_2$	4.0×10^{14}	9.8	6	−16	estimated[e]
23.	$CH_3^\bullet + Ph-CH_2CN \rightarrow Ph-CHCN^\bullet + CH_4$	5×10^{12}	9	−2	−19	estimated[f]
24.	$CH_3^\bullet + o\text{-}A_1(CN)CH_3 \rightarrow o\text{-}A_1(CN)CH_2^\bullet + CH_4$	5×10^{12}	9	−1	−17	estimated[f]
25.	$CH_3^\bullet + m\text{-}A_1(CN)CH_3 \rightarrow m\text{-}A_1(CN)CH_2^\bullet + CH_4$	5×10^{12}	9	−1	−17	estimated[f]
26.	$CN^\bullet + Ph-CH_2CN \rightarrow Ph-CHCN^\bullet + HCN$	2.0×10^{13}	2.3	2	−38	estimated[g]
27.	$CN^\bullet + o\text{-}A_1(CN)CH_3 \rightarrow o\text{-}A_1(CN)CH_2^\bullet + HCN$	2.0×10^{13}	2.3	3	−36	estimated[g]
28.	$CN^\bullet + m\text{-}A_1(CN)CH_3 \rightarrow m\text{-}A_1(CN)CH_2^\bullet + HCN$	2.0×10^{13}	2.3	3	−36	estimated[g]
29.	$CH_2CN^\bullet + Ph-CH_2CN \rightarrow Ph-CHCN^\bullet + CH_3CN$	1×10^{12}	9	−2	−6	estimated
30.	$CH_2CN^\bullet + o\text{-}A_1(CN)CH_3 \rightarrow o\text{-}A_1(CN)CH_2^\bullet + CH_3CN$	1×10^{12}	9	−2	−3	estimated
31.	$CH_2CN^\bullet + m\text{-}A_1(CN)CH_3 \rightarrow m\text{-}A_1(CN)CH_2^\bullet + CH_3CN$	1×10^{12}	9	−2	−3	estimated
32.	$C_3H_3^\bullet + Ph-CH_2CN \rightarrow Ph-CHCN^\bullet + C_3H_4$	1×10^{12}	9	−1	−5	estimated
33.	$C_3H_3^\bullet + o\text{-}A_1(CN)CH_3 \rightarrow o\text{-}A_1(CN)CH_2^\bullet + C_3H_4$	1×10^{12}	9	0	−2	estimated
34.	$C_3H_3^\bullet + m\text{-}A_1(CN)CH_3 \rightarrow m\text{-}A_1(CN)CH_2^\bullet + C_3H_4$	1×10^{12}	9	0	−2	estimated
35.	$H^\bullet + Ph-CH_2CN \rightarrow Ph-CH_2^\bullet + HCN$	4×10^{14}	6	8	−15	estimated
36.	$H^\bullet + o\text{-}A_1(CN)CH_3 \rightarrow Ph-CH_2^\bullet + HCN$	2×10^{14}	12	8	−17	estimated[h]
37.	$H^\bullet + m\text{-}A_1(CN)CH_3 \rightarrow Ph-CH_2^\bullet + HCN$	2×10^{14}	12	8	−16	estimated[h]
38.	$CH_3^\bullet + Ph-CH_2CN \rightarrow Ph-CH_2^\bullet + CH_3CN$	5×10^{12}	6	1	−8	estimated
39.	$CH_3^\bullet + o\text{-}A_1(CN)CH_3 \rightarrow Ph-CH_2^\bullet + CH_3CN$	5×10^{12}	12	2	−10	estimated
40.	$CH_3^\bullet + m\text{-}A_1(CN)CH_3 \rightarrow Ph-CH_2^\bullet + CH_3CN$	5×10^{12}	12	1	−9	estimated
41.	$CN^\bullet + Ph-CH_2CN \rightarrow Ph-CH_2^\bullet + C_2N_2$	2×10^{13}	3	1	−23	estimated[i]
42.	$CN^\bullet + o\text{-}A_1(CN)CH_3 \rightarrow Ph-CH_2^\bullet + C_2N_2$	2×10^{13}	3	2	−25	estimated[i]
43.	$CN^\bullet + m\text{-}A_1(CN)CH_3 \rightarrow Ph-CH_2^\bullet + C_2N_2$	2×10^{13}	3	2	−24	estimated[i]
44.	$H^\bullet + Ph-CH_2CN \rightarrow C_6H_6 + CH_2CN^\bullet$	5×10^{13}	5	5	−20	estimated[j]
45.	$H^\bullet + Ph-CH_2CN \rightarrow Ph-CH_3 + CN^\bullet$	2×10^{14}	19	4	17	estimated[k]
46.	$H^\bullet + o\text{-}A_1(CN)CH_3 \rightarrow Ph-CH + CH_3^\bullet$	5×10^{13}	5	6	−13	estimated[j]

TABLE 3 (Continued)

	reaction	A	E_{activ}	$\Delta S_r°$	$\Delta H_r°$	source
47.	$H^\bullet + o\text{-}A_1(CN)CH_3 \rightarrow Ph\text{-}CH_3 + CN^\bullet$	2×10^{14}	17	5	15	estimated[k]
48.	$H^\bullet + m\text{-}A_1(CN)CH_3 \rightarrow Ph\text{-}CN + CH_3^\bullet$	5×10^{13}	5	6	−12	estimated[j]
49.	$H^\bullet + m\text{-}A_1(CN)CH_3 \rightarrow Ph\text{-}CH_3 + CN^\bullet$	2×10^{14}	17	5	16	estimated[k]
50.	$CH_3^\bullet + Ph\text{-}CH_2CN \rightarrow Ph\text{-}CH_3 + CH_2CN^\bullet$	5×10^{12}	5	1	−8	estimated
51.	$CN^\bullet + Ph\text{-}CH_2CN \rightarrow Ph\text{-}CN + CH_2CN^\bullet$	5×10^{13}	2	3	−36	estimated
52.	$CN^\bullet + o\text{-}A_1(CN)CH_3 \rightarrow C_6H_4CN^\bullet + CH_3CN$	5×10^{13}	2	4	−19	estimated
53.	$CN^\bullet + m\text{-}A_1(CN)CH_3 \rightarrow C_6H_4CN^\bullet + CH_3CN$	5×10^{13}	2	4	−19	estimated
54.	$C_8H_6N^\bullet \rightarrow Ph\text{-}CHCN^\bullet$	2.3×10^{14}	72	6	4	estimated[l]
55.	$C_8H_6N^\bullet \rightarrow A_1(NC)CH_2^\bullet$	8.0×10^{14}	62	7	28	estimated[l]
56.	$A_1(NC)CH_2^\bullet \rightarrow o\text{-}A_1(CN)CH_2^\bullet$	5.9×10^{14}	36	−1	−20	estimated[l]
57.	$A_1(NC)CH_2^\bullet \rightarrow m\text{-}A_1(CN)CH_2^\bullet$	8.0×10^{13}	47	−1	−21	estimated[l]
58.	$(C_8H_6N^\bullet \rightarrow C_5H_4\text{-}CCH^\bullet + HCN)$	6×10^{14}	75	49	75	estimated
59.	$(C_8H_6N^\bullet \rightarrow C_5H_4CN^\bullet + C_2H_2)$	6×10^{14}	75	50	72	estimated
60.	$Ph\text{-}CH_2^\bullet \rightarrow C_5H_5^\bullet + C_2H_2$	4.0×10^{14}	78	39	68	estimated[m]
61.	$Ph\text{-}CHCN^\bullet \rightarrow C_5H_5^\bullet + HCCCN$	4.0×10^{14}	78	37	71	estimated[m]
62.	$Ph\text{-}CHCN^\bullet \rightarrow C_5H_4CN^\bullet + C_2H_2$	4.0×10^{14}	78	44	68	estimated[m]
63.	$o\text{-}A_1(CN)CH_2^\bullet \rightarrow C_5H_5^\bullet + HCCN$	4.0×10^{14}	78	37	67	estimated[m]
64.	$o\text{-}A_1(CN)CH_2^\bullet \rightarrow C_5H_4CN^\bullet + C_2H_2$	4.0×10^{14}	78	44	64	estimated[m]
65.	$m\text{-}A_1(CN)CH_2^\bullet \rightarrow C_5H_5^\bullet + HCCCN$	4.0×10^{14}	78	37	67	estimated[m]
66.	$m\text{-}A_1(CN)CH_2^\bullet \rightarrow C_5H_4CN^\bullet + C_2H_2$	4.0×10^{14}	78	44	65	estimated[m]
67.	$C_6H_4N^\bullet \rightarrow C_3H_3^\bullet + HCCCN$	4.0×10^{14}	77	36	76	estimated
68.	$C_5H_4CN^\bullet + H^\bullet \rightarrow C_5H_5CN$	1×10^{14}	0.0	−34	−82	estimated
69.	$C_5H_5^\bullet \rightarrow C_3H_3^\bullet + C_2H_2$	1×10^{14}	75	43	73	estimated
70.	$C_5H_6 \rightarrow C_5H_5^\bullet + H^\bullet$	1.1×10^{15}	77.0	34	86	31.
71.	$C_5H_5^\bullet + C_2H_2 \rightarrow C_5H_5\text{-}CCH + H^\bullet$	3×10^{12}	25	−5	22	estimated
72.	$C_5H_4\text{-}CCH^\bullet \rightarrow C_4H_2 + C_3H_3^\bullet$	4×10^{14}	78	41	76	estimated
73.	$C_5H_4\text{-}CCH^\bullet + H^\bullet \rightarrow C_5H_5\text{-}CCH$	1×10^{14}	0	−34	−86	estimated
74.	$C_5H_5\text{-}CCH + H^\bullet \rightarrow C_5H_4\text{-}CCH^\bullet + H_2$	4×10^{14}	5	6	−21	estimated
75.	$Ph\text{-}CN \rightarrow C_6H_4CN^\bullet + H^\bullet$	7.59×10^{15}	106.0	35	113	30
76.	$Ph\text{-}CN + H^\bullet \rightarrow C_6H_4CN^\bullet + H_2$	1.0×10^{14}	16.0	8	6	30
77.	$Ph\text{-}CN + H^\bullet \rightarrow Ph + HCN$	1.8×10^{14}	12.6	8	3	30
78.	$Ph\text{-}CN + H^\bullet \rightarrow C_6H_6 + CN^\bullet$	2.0×10^{14}	19.0	2	17	30
79.	$C_6H_4CN^\bullet \rightarrow l\text{-}C_7H_4N^\bullet$	1.0×10^{14}	67	14	65	30
80.	$l\text{-}C_7H_4N^\bullet + H^\bullet \rightarrow C_6H_4 + HCN$	5.0×10^{14}	40	3	−73	30
81.	$l\text{-}C_7H_4N^\bullet \rightarrow C_4H_3^\bullet + HCCCN$	2.0×10^{14}	41	33	37	30
82.	$C_6H_6 \rightarrow Ph + H^\bullet$	8.0×10^{15}	106.0	35	113	32
83.	$H^\bullet + C_6H_6 \rightarrow Ph + H_2$	1.41×10^{14}	16.0	8	6	33
84.	$Ph \rightarrow C_6H_5^\bullet$	1.0×10^{14}	67	17	63	32
85.	$C_6H_5^\bullet \rightarrow C_6H_4 + H^\bullet$	2.0×10^{14}	38	28	39	32
86.	$C_6H_5^\bullet \rightarrow C_4H_3^\bullet + C_2H_2$	5.0×10^{14}	38	35	41	32
87.	$C_4H_3^\bullet \rightarrow C_4H_2 + H^\bullet$	1.1×10^{14}	39	24	39	32
88.	$Ph + C_2H_2 \rightarrow Ph\text{-}CCH + H^\bullet$	3.6×10^{12}	8.0	−5	−4	34
89.	$Ph\text{-}CH_3 \rightarrow Ph\text{-}CH_2^\bullet + H^\bullet$	2.4×10^{15}	86.9	34	94	29
90.	$C_3H_3^\bullet + C_3H_3^\bullet \rightarrow C_6H_6$	1.0×10^{12}	0	−60	−147	35
91.	$Ar + pC_3H_4 \rightarrow C_3H_3^\bullet + H^\bullet + Ar$	1.0×10^{17}	70.0	33	93	35
92.	$CH_3^\bullet + CH_2CN^\bullet \rightarrow C_2H_3CN + H_2$	5×10^{13}	0	−8	−50	estimated
93.	$CH_3CN \rightarrow CH_2CN^\bullet + H^\bullet$	1.0×10^{15}	93.0	35	94	36
94.	$CH_3^\bullet + CH_3CN \rightarrow CH_4 + CH_2CN^\bullet$	1.0×10^{10}	0	1	−14	37
95.	$CH_3^\bullet + CH_3^\bullet \rightarrow C_2H_4 + H_2$	1.0×10^{16}	32.9	−7	−57	38
96.	$CH_3^\bullet + CH_3^\bullet \rightarrow C_2H_6$	7.0×10^{12}	0	−40	−90	39
97.	$CH_3^\bullet + H_2 \rightarrow CH_4 + H^\bullet$	$6.46 \times 10^2 \, T^{3.0}$	7.7	−7	−1	40
98.	$C_2H_5^\bullet + H^\bullet \rightarrow CH_3^\bullet + CH_3^\bullet$	3.6×10^{13}	0	5	−12	41
99.	$C_2H_6 \rightarrow C_2H_5^\bullet + H^\bullet$	4.35×10^{16}	100.2	36	102	29
100.	$CN^\bullet + H_2 \rightarrow HCN + H^\bullet$	$2.95 \times 10^6 \, T^{2.45}$	2.2	−3	−20	42
101.	$CN + CH_4 \rightarrow CH_3^\bullet + HCN$	$6.03 \times 10^4 \, T^{3.64}$	−0.4	4	−19	29
102.	$H^\bullet + CH_3CN \rightarrow CH_3^\bullet + HCN$	2.10×10^{12}	7.8	7	−7	43
103.	$H^\bullet + HCCCN \rightarrow C_2H^\bullet + HCN$	2×10^{14}	25	9	24	estimated
104.	$H^\bullet + HCCCN \rightarrow C_2H^\bullet + HCN$	2×10^{14}	25	9	24	estimated
105.	$H^\bullet + C_2H_2 \rightarrow C_2H^\bullet + H_2$	1×10^{14}	23	4	23	29
106.	$C_2H_2 + C_2H^\bullet \rightarrow C_4H_2 + H^\bullet$	1.3×10^{13}	0	−5	−20	44
107.	$HCCCN + C_2H^\bullet \rightarrow C_4H_2 + CN^\bullet$	1×10^{13}	0	2	0	estimated
108.	$pC_3H_4 + C_2H^\bullet \rightarrow C_4H_2 + CH_3^\bullet$	1×10^{15}	0	0	−28	estimated
109.	$Ph\text{-}CH_3 + C_2H^\bullet \rightarrow Ph\text{-}CCH + CH_3^\bullet$	1×10^{13}	0	2	−33	estimated

[a] $\Delta H_r°$ and $\Delta S_r°$ are expressed in units of kcal/mol and cal/(K mol), respectively. Rate constants are expressed as $k = A \exp(-E/RT)$ in units of cm³, s, mol, kcal. [b] Estimation based on pyrrole ↔ pyrolenine tautomerization (ref 5). [c] Estimation based on $CH_3NC \rightarrow CH_3CN$ isomerization (ref 29). [d] Estimation based on H-atom ejection from toluene: $Ph\text{-}CH_3 \rightarrow Ph\text{-}CH_2^\bullet + H^\bullet$ (ref 29). [e] Estimation based on H-atom abstraction from toluene: $Ph\text{-}CH_3 + H^\bullet \rightarrow Ph\text{-}CH_2^\bullet + H_2$ (ref 29). [f] Estimation based on H-atom abstraction from toluene by $CH_3^\bullet$ radical: $Ph\text{-}CH_3 + CH_3^\bullet \rightarrow Ph\text{-}CH_2^\bullet + CH_4$ (ref 29). [g] Estimation based on H-atom abstraction from methane by $CN^\bullet$ radical: $CH_4 + CN^\bullet \rightarrow CH_3^\bullet + HCN$ (ref 29). [h] Estimation based on the dissociative attachment of H atom to the $-C\equiv N$ triple bond in benzonitrile: $Ph\text{-}CN + H^\bullet \rightarrow Ph + HCN$ (ref 30). [i] Estimation based on the dissociative attachment of $CN^\bullet$ radicals to the $-C\equiv N$ triple bond in hydrogen cyanide: $HCN + CN^\bullet \rightarrow H^\bullet + C_2N_2$ (ref 29). [j] Estimation based on the methyl group displacement from toluene by H atoms: $Ph\text{-}CH_3 + H^\bullet \rightarrow C_6H_6 + CH_3^\bullet$ (refs 23 and 24). [k] Estimation based on the cyanide group displacement from benzonitrile by H atoms: $Ph\text{-}CN + H^\bullet \rightarrow C_6H_6 + CN^\bullet$ (ref 30). [l] Estimation based on the similar reactions for the corresponding stable molecules (reactions 1 and 3−5 in the present scheme). [m] Estimation based on the experimental rate constants for the total decomposition of benzyl radical: $Ph\text{-}CH_2^\bullet \rightarrow Products$ (ref 29).
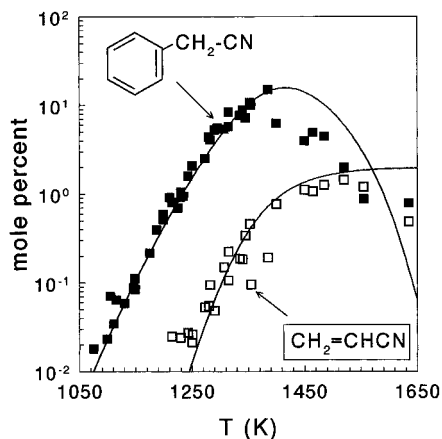
Figure 9. Comparison between experimental and calculated mole percent, of benzyl cyanide and acrylonitrile. The points are experimental mole percent and the line connects the calculated values at 25 K intervals.
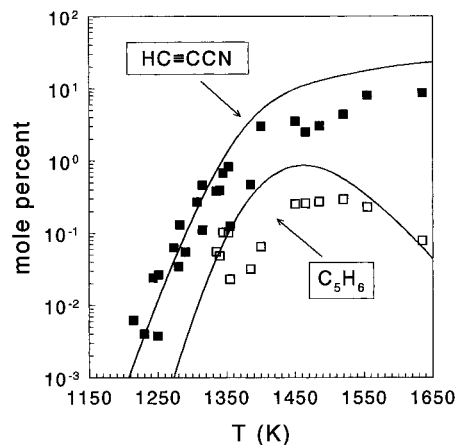

Figure 11. Comparison between experimental and calculated mole percent of cyanoacetylene and cyclopentadiene. The points are experimental mole percent and the line connects the calculated values at 25 K intervals.
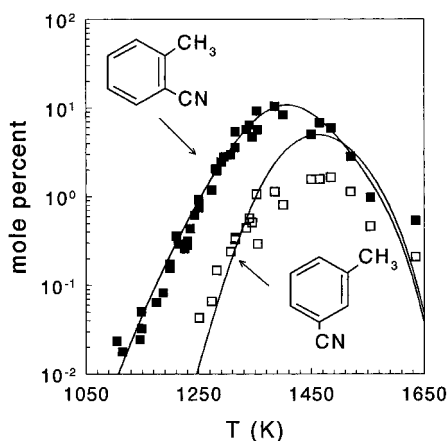

Figure 10. Comparison between experimental and calculated mole percent of *o*- and *m*-tolunitriles. The points are experimental mole percent, and the line connects the calculated values at 25 K intervals.
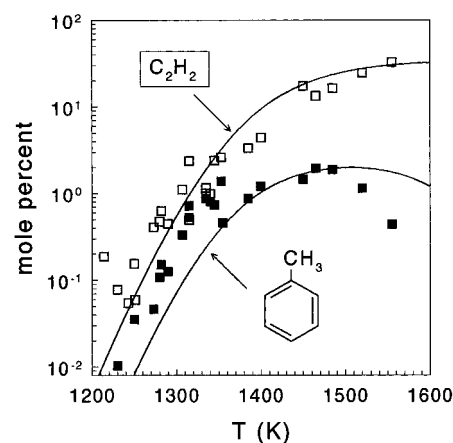

Figure 12. Comparison between experimental and calculated mole percent of acetylene and toluene. The points are experimental mole percent and the line connects the calculated values at 25 K intervals.

Figure 13. Comparison between experimental and calculated mole percent of hydrogen cyanide and phenyl acetylene. The points are experimental mole percent and the line connects the calculated values at 25 K intervals.

obtained in this investigation. Parameters for the reactions that appear in the scheme were either estimated or were taken from various literature sources mainly from the NIST-Chemical Kinetics Standard Reference Data Base.[29] The parameters for each reaction was taken as the best fit, sometimes to a large number of entries. Many of the reactions that compose the present scheme are very similar to the ones that appear in kinetic schemes that describe the decomposition of benzene,[32] benzonitrile[30] and toluene,[27,45,46] the difference being the type of substituents on the aromatic ring. The parameters for these reactions were used in the present scheme. Parameters that could not be found in available compilations were also estimated on the basis of similar reactions for which the rate parameters were known.

The thermodynamic properties of the majority of the species were taken from various literature sources.[9,47,48] The heats of formation of several species were estimated using NIST Structures and Properties program.[48]

Figures 9−19 show experimental and calculated mole percent of the reaction products. The lines pass through calculated points at 25 K intervals. As can be seen, the overall agreement is quite satisfactory.

Table 4 shows the sensitivity spectrum of the reaction scheme for the major reaction products at 1150 and 1350 K, respectively. The sensitivity factor $S_{i,j}$ is defined in the table as $\Delta\log C_i/\Delta\log k_j$ at $t = 2$ ms. $S_{i,j} = 1$ means that a factor of 2 change in k_j will cause a factor of 2 change in C_i. $S_{i,j}$ was evaluated by changing k_j by a factor of 2. Reactions for which $S_{i,j}$ is less than 0.1 for all the products both at low and at high temperature are not included in the table. At large, the spectrum is self-evident. The following is a brief discussion on some of the features of the sensitivity analysis.

Reaction 1, the isomerization of indole to benzyl cyanide, in addition to its effect on benzyl cyanide itself, it strongly affects the products that are formed from the latter as a precursor. These are toluene, phenylacetylene, and to a lesser extent, also HCN.

Isomerization and Decomposition of Indole

J. Phys. Chem. A, Vol. 101, No. 42, 1997 **7799**

Figure 14. Comparison between experimental and calculated mole percent of C_4H_2. The points are experimental mole percent, and the line connects the calculated values at 25 K intervals.

Figure 15. Comparison between experimental and calculated mole percent of benzonitrile. The points are experimental mole percent, and the line connects the calculated values at 25 K intervals. The dashed line shows calculated mole percent without dissociative attachment of H atoms to indole to form benzonitrile and methyl radical.

Figure 16. Comparison between experimental and calculated mole percent of benzene. The points are experimental mole percent and the line connects the calculated values at 25 K intervals. The dashed line shows calculated mole percent without dissociative attachment of H-atoms to indole to form benzene and cyanomethyl radical.

The production of tolunitriles involves three consecutive steps. Steps 2, 3, and 4 for *o*-tolunitrile and steps 2, 3, and 5 for *m*-tolunitrile (Table 3). As can be seen in Table 4, step 2 is not among the reactions that affect the production of the latter. The reason is that the reverse rate of reaction 2 is by an order of magnitude faster than the forward rate constant of reaction 3 so that reaction 2 reaches thermal equilibrium as of the early
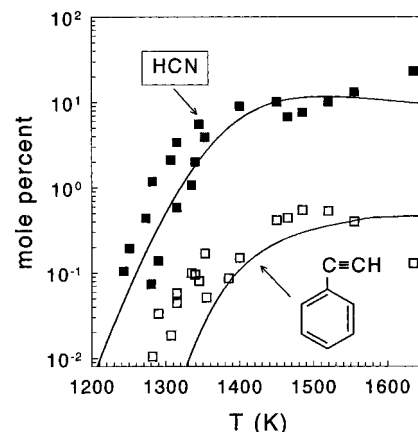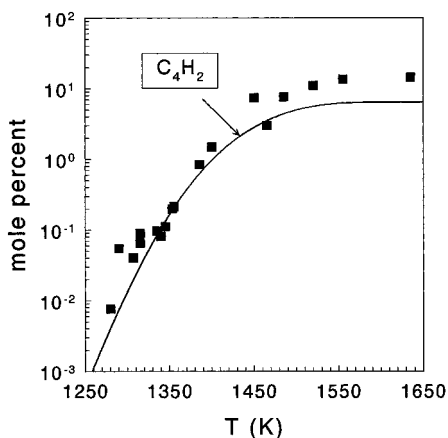

Figure 17. Comparison between experimental and calculated mole percent of acetonitrile. The points are experimental mole percent, and the line connects the calculated values at 25 K intervals.

Figure 18. Comparison between experimental and calculated mole percent of methane. The points are experimental mole percent, and the line connects the calculated values at 25 K intervals.

Figure 19. Comparison between experimental and calculated mole percent of cyclopentadienyl cyanide. The points are experimental mole percent, and the line connects the calculated values at 25 K intervals.

stages of the reaction. This implies that only the equilibrium concentration of indolenine plays a role in this isomerization and increasing the rate of reaction 2 has no effect on the production rate of the tolunitriles. Reaction 3 is rate determining and affects both isomers. Reactions 4 and 5 are in competition to which the concentration of *m*-tolunitrile is more sensitive.

Reaction 6 is responsible for the initiation of the free radical reactions. The entire plethora of decomposition products is enhanced by increasing k_6. This reduces to some extent the

TABLE 4: Sensitivity Factors $S_{ij} = \Delta \log C_i/\Delta \log k_j$ at 1150/1350 K, k Is Changed by a Factor of 2

reaction number	CH$_4$	C$_2$H$_2$	HCN	CH$_3$CN	C$_4$H$_2$	HCCCN	C$_2$H$_3$CN	C$_5$H$_6$	C$_6$H$_6$	C$_5$H$_5$–C≡CH	C$_5$H$_5$–CN	Ph–CH$_3$	Ph–C≡CH	Ph–CN	Ph–CH$_2$CN	o-A$_1$(CN)CH$_3$	m-A$_1$(CN)CH$_3$
1	–/–0.38	–/–0.06	0.16/0.14	–/0.23	–/–0.05	–/–0.05	–/–0.27	–/–0.17		–/–0.22	–/–0.23	0.98/0.45	0.68/0.62	–/–0.17	0.99/0.92	–/–0.07	–/–0.07
3									–/–0.06	–/–0.06	–/–0.07					0.96/0.72	0.96/0.55
4																	–0.51/–
5																–/–0.10	0.98/0.64
6	0.97/0.43	0.98/0.53	0.98/0.51	0.96/0.20	0.98/0.44	0.98/0.46	1.94/0.93	1.96/1.01	0.98/0.52	1.96/1.01	1.96/1.06	0.97/0.49	2.08/0.65	0.98/0.53	–/–0.22	–/–0.09	–/–0.31
10													0.68/0.70				
13	–0.76/–0.49	–0.08	–0.06/–	–0.76/–0.43	–/0.11	–/0.08	–1.51/–0.92	–0.74/–0.38	–0.76/–0.56	–0.74/–0.29	–0.74/–0.34	–0.76/–0.60	–0.40/–0.14	–0.76/–	–0.56		–/–0.07
14	0.75/0.76			–0.23/–			0.59/0.49	–0.25/–0.15	–0.23/–0.20	–0.25/–0.15	–0.25/–0.15	0.73/0.49	0.18/0.20	0.75/0.72			
15	–0.14/–0.30			0.86/0.59			0.71/0.43	–0.15/–0.10	0.86/0.75	–0.15/–0.09	–0.15/–0.10	–0.14/–0.27	–0.07/–	–0.12/–0.12			
16	–/0.31			0.24/–			–0.97/–0.51					–0.94/–0.36					
17							–0.74/–0.45										
35			0.16/0.21	–/–0.06			–/–0.07	–/–0.06	–/–0.06	–/–0.07	–/–0.09	–/0.19					
38	–/–0.09			–/0.15			–/–0.09										
44				–/0.11			–/–0.07		–/–0.16			–/–0.06					
50	–/–0.15			–/–0.12								0.98/0.50					
55					–0.07/–	0.18/–		0.24/–		–0.07/–	–0.06/–		–0.06				
58		–/–0.10	0.90/0.70		0.99/0.88	–/–0.10		–/–0.10		0.99/0.87	–/–0.12		–/–0.15				
59		0.94/0.57	–/–0.09		–/–0.10			–/–0.09		–/–0.10	0.95/0.61		0.95/0.52				
61						–/0.14		–/0.14									
63						0.97/0.43		0.98/0.58									
64		0.08/0.19									0.07/0.21		0.08/0.18				
65								–0.33									
66		–/0.14									–/0.12		–0.11				
67						–/0.18					–/–0.07						
68											0.99/0.37						
70								0.99/0.73									
72					0.99/0.90					–/–0.07							
73					–/–0.09					0.99/0.61							
77													0.44/0.29				
82													–/–0.22				
88													0.99/0.85				
89												–/–0.30					
92	–/–0.15			–/–0.27								–/–0.10					

Isomerization and Decomposition of Indole

J. Phys. Chem. A, Vol. 101, No. 42, 1997 **7801**

production of the isomers owing to competition with the dissociation. Reaction 13, on the other hand, can be considered as a free radical scavenging reaction. It replaces H atoms by a much less reactive radical. This reaction inhibits the fragmentation process wherever the concentration of the reactant is still high enough.

As has been suggested before, the relatively high concentrations of benzene and benzonitrile at low temperatures can be explained by a direct attack of H atoms on the reactant molecule. To clarify this point, we ran the kinetic scheme without reactions 14 and 15. The results are shown in Figures 15 and 16. It can readily be seen that the concentrations of both benzene and benzonitrile cannot be accounted for by consecutive reactions but only by an attack on the reactant.

V. Conclusion

The thermal reactions of indole are dominated by isomerizations to three isomers at low temperatures (small conversion) and by fragmentation as the temperature increases. The existence of a fast indole ↔ indolenine tautomerism is necessary to explain some of the isomerizations. The ejection of an sp^3 H atom by breaking either a N−H bond in indole or a C−H bond in indolenine initiates the free radical reactions in the system.

References and Notes

(1) Attar, A.; Hendrickson, G. G. In *Coal Structure*; Meyers, R. A., Ed.; Academic Press: New York, 1982; p 132.

(2) Given, P. H. In *Coal Science*; Gorbaty, M. L., Larsen, J. W., Wender, I., Eds.; Academic Press: New York, 1982; Vol. 3, p 65.

(3) Unsworth, J. F. In *Coal Quality and Combustion Performance*; Unsworth, J. F., Barrat, D. J., Roberts, P. T., Eds.; Elsevier Science Publishers: Amsterdam, 1991; Chapter 4.2, p 206.

(4) Lifshitz, A.; Tamburu, C.; Suslensky, A. *J. Phys. Chem.* **1989**, *93*, 5802.

(5) Mackie, J. C.; Colket, M. B., III; Nelson, P. F.; Esler, M. *Int. J. Chem. Kinet.* **1991**, *23*, 733.

(6) Bruinsma, O. S. L.; Tromp, P. J. J.; de Sauvage Nolting, H. J. J.; Moulijn, J. A. *Fuel* **1988**, *67*, 334.

(7) Julian, P. L.; Meyer, E. W.; Printy, H. C. *The Chemistry of Indole* in *Heterocyclic Compounds*; Elderfield, R. C., Ed.; John Wiley & Sons, Inc.: New York, 1952; Vol. 3, pp 74−83.

(8) Sumpter, W. C.; Miller, F. M. *Heterocyclic Compounds with Indole and Carbazole Systems*; Interscience Publishers, Inc.: New York, 1954; pp 25−28.

(9) Burcat, A.; McBride, B. *1995 Ideal Gas Thermodynamics Data for Combustion and Air-Pollution Use*; Technion−Israel Institute of Technology: Tel Aviv, 1995.

(10) Rogers, A. S.; Ford, W. C. F. *Int. J. Chem. Kinet.* **1973**, *5*, 965.

(11) Lifshitz, A.; Tamburu, C.; Frank, P.; Just, Th. *J. Phys. Chem.* **1993**, *97*, 4085.

(12) Kiefer, J. H.; Shah, J. N. *J. Phys. Chem.* **1987**, *91*, 3024.

(13) Troe, J. *J. Chem. Phys.* **1977**, *66*, 4745, 4758.

(14) Gilbert, R. G., Luther, K.; Troe, J. *Ber. Bunsen-Ges. Phys. Chem.* **1983**, *87*, 169.

(15) Gardiner, W. C., Jr.; Troe, J. In *Combustion Chemistry*; Gardiner, W. C., Jr., Ed.; Springer-Verlag, Inc: New York, 1984; Chapter 4, p 173.

(16) Collier, W. B.; Klots, T. D. *Spectrochim. Acta, Part A* **1995**, *51*, 1255.

(17) Morrison, R. Th.; Boyd, R. N. *Organic Chemistry*; Allyn and Bacon, Inc.: Boston, 1976; p 1009

(18) Lifshitz, A.; Bidani, M.; Bidani, S. *J. Phys. Chem.* **1986**, *90*, 5373.

(19) Wohlfeiler, D., Ph.D. Thesis, submitted to the Senate of the Hebrew University, Jerusalem, 1992.

(20) Lifshitz, A.; Wohlfeiler, D. *J. Phys. Chem.* **1992**, *96*, 4505.

(21) Laskin, A.; Lifshitz, A. In *Proceeding of the 20th Symposium on Shock Tubes and Waves, Pasadena, USA 1995*; Sturtevant, B., Shepherd, J. E., Hornung, H., Eds.; World Scientific: London, 1996; p 971

(22) Lifshitz, A.; Tamburu, C.; Shashua, R. *J. Phys. Chem.* **1997**, *101*, 1018.

(23) Robaugh, D.; Tsang, W. *J. Phys. Chem.* **1986**, *90*, 4159.

(24) Manion, J. A.; Louw, R. *J. Phys. Chem.* **1990**, *94*, 4127.

(25) Smith, R. D. *J. Phys. Chem.* **1979**, *83*, 1553.

(26) Smith, R. D. *Combust. Flame* **1979**, *35*, 179.

(27) Braun-Unkhoff, M.; Frank, P.; Just, Th. In *22th Symposium (International) on Combustion*; The Combustion Institute: Pittsburgh, PA, 1988; p 1053.

(28) Burcat, A.; Dvinyaninov, M. *Int. J. Chem. Kinet.* **1997**, *29*, 505.

(29) Westly, F.; Herron, J. T.; Cvetanovich, R. J.; Hampson, R. F.; Mallard, W. G. *NIST-Chemical Kinetics Standard Reference Data Base 17,* Version 5.0; National Institute of Standards and Technology: Washington, DC.

(30) Lifshitz, A.; Cohen, Y.; Braun-Unkhoff, M.; Frank, P. *26th Symposium (International) on Combustion;* The Combustion Institute: Pittsburgh, PA, 1996; p 659.

(31) Roy, K.; Frank, P.; Just, Th. *Is. J. Chem.* **1996**, *36*, 275.

(32) Laskin, A.; Lifshitz, A. *26th Symposium (International) on Combustion;* The Combustion Institute: Pittsburgh, PA, 1996; p 669.

(33) Kiefer, J. H.; Mizerka, L. J.; Patel, M. R.; Wei, H. C. *J. Phys. Chem.* **1985**, *89*, 2013.

(34) Hertzler, J.; Frank, P. *Ber. Bunsen-Ges. Phys. Chem.* **1992**, *96*, 1333.

(35) Wu, C. H.; Kern, R. D. *J. Phys. Chem.* **1987**, *91*, 6291.

(36) Lifshitz, A.; Tamburu, C.; Carroll, H. F. *Int. J. Chem. Kinet.* **1997**, in press.

(37) Metcalfe, E.; Booth, D.; McAndrey, H.; Wooley, W. D. *Fire Mater.* **1983**, *7*, 185.

(38) Kern, R. D.; Singh, H. J.; Wu, C. H. *Int. J. Chem. Kinet.* **1988**, *20*, 731.

(39) Clark, T. C.; Izod, P. J.; Valentin, M. A. D.; Dove, J. E. *J. Chem. Phys.* **1970**, *53*, 2982.

(40) Warnatz, J. *Rate Coefficients in the C/H/O System* in *Combustion Chemistry;* Gardiner, W. C., Jr., Ed.; Springer-Verlag, Inc.: New York, 1984; p 197.

(41) Tsang, W.; Hampson, R. F. *J. Phys. Chem. Ref. Data* **1986**, *15*, 1087.

(42) Wagner, A. F.; Bair, R. A. *Int. J. Chem. Kinet.* **1986**, *18*, 473.

(43) Jamieson, j. W. S.; Brown, G. R.; Tanner, J. S. *Can. J. Chem.* **1970**, *48*, 3619.

(44) Laufer, A. H.; Bass, A. M. *J. Phys. Chem.* **1979**, *83*, 310.

(45) Pamidimukkala, K. M.; Kern R. D.; Patel, M. R.; Wei, H. C.; Kiefer, J. H. *J. Phys. Chem.* **1987**, *91*, 2148.

(46) Brouwer, L. D.; Muller-Markgraf, W.; Troe, J. *J. Phys. Chem.* **1988**, *92*, 4905.

(47) Stull, D. R.; Westrum, E. F., Jr.; Sinke, G. C. *The Chemical Thermodynamics of Organic Compounds*; John Wiley & Sons: New York, 1969.

(48) Stein, S. E.; Rukkers, J. M.; Brown, R. L. *NIST-Standard Reference Data*, National Institute of Standards and Technology, Washington, DC, 1993; Vol. 25, 1993.

(49) Estimation based on the equivalent reaction in indene ($\Delta H = 104$ kcal/mol), which is very similar to indole: